Scientific Research Publishing

Open Journal of Applied Sciences, 2026, 16(5), 1812-1827
https://www.scirp.org/journal/ojapps
ISSN Online: 2165-3925
ISSN Print: 2165-3917

Indirect Solar Drying of Bananas: Correlation between Experimental Data and Drying Kinetics Models

Waly Faye[1], Mamadou Lamine Coly[2], Mamadou Seck Gueye[2], Bou Counta Mbaye[1], Omar Ngor Thiam[1], Mamadou Lamine Sow[1]

[1]Fluid Mechanics and Applications Laboratory, Cheikh Anta Diop University, Dakar, Senegal
[2]Semiconductor and Solar Energy Laboratory, Cheikh Anta Diop University, Dakar, Senegal
Email: mamadouatiamine@gmail.com

How to cite this paper: Faye, W., Coly, M.L., Gueye, M.S., Mbaye, B.C., Thiam, O.N. and Sow, M.L. (2026) Indirect Solar Drying of Bananas: Correlation between Experimental Data and Drying Kinetics Models. *Open Journal of Applied Sciences*, **16**, 1812-1827.
https://doi.org/10.4236/ojapps.2026.165100

Received: April 8, 2026
Accepted: May 23, 2026
Published: May 26, 2026

Abstract

Bananas are among the most widely consumed fruits in the world, providing calories and metabolizable vitamins for humans, as well as many other benefits. However, this fruit tends to be easily degraded by microorganisms and other chemical agents due to its high-moisture content. The study seeks to propose a practical and appropriate solution to extend the shelf life of bananas while optimizing the drying process in tropical conditions, with a focus on the accuracy of prediction models and the efficiency of solar dryers. Banana samples are dried experimentally to compare indirect solar drying with open-air drying. The experimental curves representing the reduced moisture content as a function of drying time are approximated using empirical or semi-empirical models taken from the literature. Criteria for models election were defined, and the Page and Two-Term models satisfactorily predicted the behavior of the banana samples in the dryer and the banana samples in the open air, respectively. With correlation coefficients of 0.99447, 0.99567, 0.99524, 0.98973, and 0.98962, respectively. The effective diffusivity was determined graphically by approximating the experimental results with the logarithm of the CRANK solution on the diffusive model and the logarithm of the humidity.

Keywords

Drying Solar, Reduced Humidity, Effective Diffusivity, Drying Kinetics

1. Introduction

Drying is one of the oldest food preservation techniques, aimed at reducing the moisture content of products to limit microbial growth and extend their shelf life.

Widely used in the food industry, traditional open-air drying has limitations in terms of hygiene and control of conditions, which has led to the development of modern methods such as drag drying, where a gas (often air) facilitates the removal of water through evaporation [1]. This process is particularly well-suited to hygroscopic products like bananas, whose structure undergoes a shrinkage that affects heat and mass transfer [2]. Several studies have led to a better understanding of the drying kinetics of tropical fruits. The work of Jannot *et al.* [3] established mathematical models linking water loss to the variation in volume and density of bananas during drying at temperatures of 40˚C, 50˚C, and 60˚C. Similarly, research on sorption isotherms [4] [5] and temperature-jump drying kinetics [6] has provided tools for predicting banana behavior. However, few studies have focused on applying empirical models to optimize forced convection drying, taking into account effective diffusivity and the influence of temperature. Bananas, a hygroscopic fruit rich in nutrients (fiber, potassium, vitamins) and bioactive compounds (dopamine, catechin) [7], are a product of interest to the food industry due to their nutritional value and growing popularity [2] [3]. Optimizing their drying process would improve the quality of dehydrated products while reducing energy costs. This study aims to experimentally analyze the drying kinetics of bananas using an indirect forced convection rack dryer, to evaluate the influence of temperature on these kinetics, to select a suitable empirical model from those available in the literature, and to determine the effective diffusivity of the samples. These results will contribute to improving the prediction and optimization of banana drying processes, with potential applications in the food industry.

2. Theoretical Analysis

2.1. Variation in Dry Base Moisture Content

It consists of monitoring the wet mass $Mh(t)$ of the product to be dried as a function of time by successive weighings until a constant value is reached. Thus, the final mass m_s is obtained after 24 hours in an oven at 102˚C [6] [8].

$$X(t) = \frac{m_i - m_s}{m_i} \tag{1}$$

2.2. Determination of Equilibrium Moisture Content

The mass of each sample is measured regularly, allowing the equilibrium moisture content to be determined using the following relationship [9] [10]:

$$X_e = \frac{m_{eq} - m_s}{m_s} \tag{2}$$

where X_e is the equilibrium moisture content, m_{eq} is the mass of the sample at equilibrium and m_s is the anhydrous mass.

2.3. Reduced Humidity

This is the ratio of the change in moisture content at time t to the change at equilibrium, divided by the ratio of the change in initial moisture content to the change at equilibrium, given by Equation (3) [11].

$$X^* = \frac{X(t) - X_e}{X_0 - X_e} \tag{3}$$

2.4. Mathematical Models

Several empirical or semi-empirical models are used to describe drying kinetics and predict the reduced moisture content X_r as a function of banana drying time. These models are defined in **Table 1** [6] [8] [9] [12]. This smoothing was performed using the Levenberg-Marquard nonlinear regression method on Origin Pro 9.

Table 1. Mathématiques models.

Nom du modèle	Expression
Newton	$X_r = \exp(-kt)$
Page	$X_r = \exp(-kt^n)$
Page modifié	$X_r = \exp\left(-(kt)^n\right)$
Logarithmique	$X_r = a\exp(-kt) + c$
Wang and Singh	$X_r = 1 + at + bt^2$
Two-Term	$X_r = a\exp(-kt) + b\exp(-gt)$
Verna *et al.*	$X_r = a\exp(-kt) + (1-a)\exp(-gt)$
Midilli-Kucuk	$X_r = a\exp(-kt^n) + bt$
Henderson et Pabis	$X_r = a\exp(-kt)$

2.5. Statistical Analysis

Nonlinear least-squares regression was used to evaluate the model parameters. The goodness of fit was determined using the statistical parameters (R^2, ESM, χ^2). [8] [13]-[15].

These parameters can be described in the following equations:

Correlation coefficient (R^2) given by Equation (4).

$$R^2 = \frac{\sum_{i=1}^{N}\left(X_{rpre,i} - X_{reexp,i}\right)^2}{\sum_{i=1}^{N} X_{rexp,i}^2} \tag{4}$$

Mean systematic error (MSE) defined by Equation (5).

$$\mathrm{ESM} = \frac{1}{N}\sum_{i=1}^{N}\left(X_{rpre,i} - X_{rexp,i}\right) \tag{5}$$

χ-reduced square given by Equation (6).

$$\chi^2 = \frac{\sum_{i=1}^{N}\left(X_{rpre,i} - X_{rexp,i}\right)^2}{N - Z} \tag{6}$$

Modeling the drying behavior of various agricultural products often requires statistical methods such as regression and correlation analysis. Regression analysis was performed using Origin Pro software and Python. The correlation coefficient (R) was the primary criterion for selecting the best equation to describe the drying curve. In addition to R, calculations of the values of and ESM were used to justify the choice of model. The higher the R values, and the higher the values of and the lower the RMSE or ESM, the better the model. These statistical parameters can be calculated as in Equations (4)-(6).

2.6. Determination of the Effective Diffusion Coefficient

Water migrates from the interior to the surface of the product under the action of various mechanisms that can combine. A simple diffusion model, based on Fick's second law, is considered for the evolution of moisture content as a function of the moisture content gradient and an overall diffusivity that encompasses the different transport phenomena. [6]

$$\frac{\partial X}{\partial t} = D_{eff} \nabla^2 X \tag{7}$$

This mathematical equation, which describes the drying process and calculates the diffusion coefficient, is based on the classic simplifying assumptions [8]:

- Water migration occurs only through diffusion;
- The moisture content at the surface is equal to that of equilibrium;
- The diffusion coefficient and the temperature of the product are considered constant;
- Sample removal is negligible.

Based on these assumptions, the analytical solution to Fick's second law, developed by Crank, 1975, can be expressed as:

$$X_r = \frac{8}{\pi^2} \sum_{n=0}^{\infty} \frac{1}{(2n-1)^2} \exp\left[-(2n-1)^2 \frac{\pi^2 D_{eff} t}{L^2}\right] \tag{8}$$

Only the first term of this equation can be used to estimate the effective moisture diffusivity for long drying times:

$$X_r = \frac{8}{\pi^2} \exp\left(-\frac{\pi^2 D_{eff} t}{L^2}\right) \tag{9}$$

With L being the thickness of the samples (m) and n a positive integer. The values of are generally determined graphically by representing the experimental drying data in terms of ln as a function of the drying time (t). $D_{eff} X_r$

$$\ln(X_r) = \ln\left(\frac{8}{\pi^2}\right) - \frac{\pi^2 D_{eff} t}{L^2} \tag{10}$$

Calculating the slope:

The effective diffusivity in a drying cylindrical object (such as a banana) is generally obtained using Fick's solution (first term):

$$\ln\left(X_r\right) = \ln\left(\frac{X(t)}{X_i}\right) \approx -\left(\frac{\pi^2}{4L^2} D_{eff}\right) t \quad (11)$$

The result is a straight line with a slope which allows the effective diffusion coefficient to be calculated, typically determined as follows: [7] $D_{eff}\pi^2 / L^2$

$$D_{eff} = -\frac{4L^2}{\pi^2}.pente \quad (12)$$

3. Materials and Methods

The aim of this article is to conduct an experimental study and model the drying kinetics of banana pulp using an indirect solar dryer. By measuring operational parameters such as temperature, humidity, and drying rate, our objective is to determine the optimal model to describe the drying kinetics of these fruits. These results will contribute to a better understanding of the potential benefits of this sustainable technology in the food industry, thereby promoting increased valorization of banana-derived products.

3.1. Experimental Setup

Our device is an indirect solar dryer with forced convection and air recirculation (**Figure 1**). This locally designed prototype solar dryer uses forced convection and an air recirculation system. It consists of the following components:

- A flat plate collector: Efficiently converts solar energy, heating the air through the greenhouse effect. A fan integrated into the collector ensures continuous circulation of the heated air towards the drying chamber, promoting even and controlled drying.
- A drying booth. It contains three horizontal racks for placing the products to be dried (**Figure 2**). Heated air circulates through the products in a forced manner.

A data acquisition device: This is a computer workstation for recording data and controlling the process.

Figure 1. Indirect solar dryer with forced convection.

Figure 2. View inside the drying room.

3.2. Equipment and Measurement

In the framework of this study, we used the following measuring instruments to carry out our experiments. The characteristics of these devices as well as their uncertainty ranges are presented in Table 2.

Table 2. Characteristics of measuring instruments.

Instruments	Measures	Measurement range	Precision
Thermocouples	Air temperature/Product temperature	0˚C to 1100˚C	2.2% to 0.75%
Thermochrons	Air temperature	−20˚C to 85˚C	0.5˚C
	Relative humidity of the air	0% - 100%	5%
Micro-manometer	Airflow	0.0001 to 1.999 m^3/s	0.001 m^3/s
Pyranometer	Irradiance	0 - 2000 W/m^2	<1.5%
Balance	Sample mass	0 - 220 g	0.1 mg
Caliper	Dimension	0 - 150 mm	0.05 mm

3.3. Experimental Procedure

The tests were carried out at the EPS (Higher Polytechnic School) of Dakar during the May 2023. Sensor and product temperatures were recorded using a type K thermocouple probe connected to a computer running PicoLog temperature acquisition software. Relative humidity of the ambient air and inside the dryer was recorded using Thermochrons. Mass was measured using a KERN ABJ 220-4N analytical balance, a high-precision instrument with an accuracy of 1 mg, ideal for laboratory and industrial applications requiring reliable and precise weighing. This balance has a maximum capacity of 220 g.

A CMP21 pyranometer was used to measure the solar flux incident on the solar collector plane. A micro-manometer, positioned in the airflow, was used in the ventilation system to perform precise measurements of volumetric flow rate, temperature, and pressure variations. The bananas used belonged to a single local

Cavendish variety. All fruits came from the same commercial batch and were harvested at maturity stage 6 (uniform yellow). The bananas were washed, peeled, and cut into uniform round slices of 5 mm thickness. The initial mass of each sample was as follows: m_1 = 4.3949 g (±0.1 mg), m_2 = 5.2701 g (±0.1 mg), m_3 = 3.9399 g (±0.1 mg), m_4 = 4.4220 g (±0.1 mg), and m_5 = 4.3992 g (±0.1 mg). No pretreatment (blanching, soaking, etc.) was applied.

Five samples were selected from this batch: two were air-dried and three were placed in the solar dryer. All five samples were prepared from the same batch and dried simultaneously to eliminate the effects of time and environmental variations. Weighings were performed on the drying racks and in the dryer before the start of drying and then at 30-minute intervals during the process. The slices were randomly arranged on the different trays to minimize positional effects.

The drying experiments in the solar dryer and in open air were conducted in parallel under the same temporal conditions. Drying was performed in an indirect solar dryer consisting of a flat-plate collector and a shelf drying cabinet with three trays. The operating conditions were as follows: air temperature ranging between 30˚C and 65˚C, air velocity of 2 - 3.5 m/s, surface area of each tray = 0.5 m^2, and product loading per tray = 1 kg/tray. Ambient temperature and relative humidity varied respectively between 20˚C - 32˚C and 20% - 60% during the trials.

At the end of the drying process, the samples were placed in an oven at 105˚C for 24 hours to determine the anhydrous mass. The equilibrium moisture content was determined experimentally for each sample by continuing the drying until constant mass was achieved.

4. Results and Discussions

4.1. Authors and Affiliations

Figure 3 presents a comparative study of the drying conditions in the forced convection solar dryer versus open-air drying for bananas. At the dryer level (Trays 1, 2, and 3): The data reveals a significant temperature increase inside the solar dryer compared to the ambient temperature. The thermal profiles of the trays (Temp_Tray1, Temp_Tray2, Temp_Tray3) show maximum temperatures between 65˚C and 70˚C, while the ambient temperature (Temp_Ambient) remains below 35˚C. Outside, the ambient temperature, subject to natural diurnal variations, remains insufficient to ensure rapid drying. This limitation prolongs the drying time, exposing the products to increased risks of fermentation or microbial contamination due to slowed evaporation.

Inside the dryer, relative humidity measurements (RH_Sheet1, RH_Sheet2, RH_Sheet3) indicate a significant decrease, reaching approximately 25%. This low humidity level results from forced convection, which extracts the moisture-saturated air produced by evaporation and replaces it with drier ambient air. This phenomenon generates a marked concentration gradient between the surrounding air and the product surface, constituting the primary driving force of water evaporation. In the open air, the ambient relative humidity (RH) remains high, generally above 40% - 50%, which limits the air's capacity to absorb moisture from the products. This low concentration gradient between the air and the product surface leads to significantly slower evaporation, reducing the overall drying efficiency.

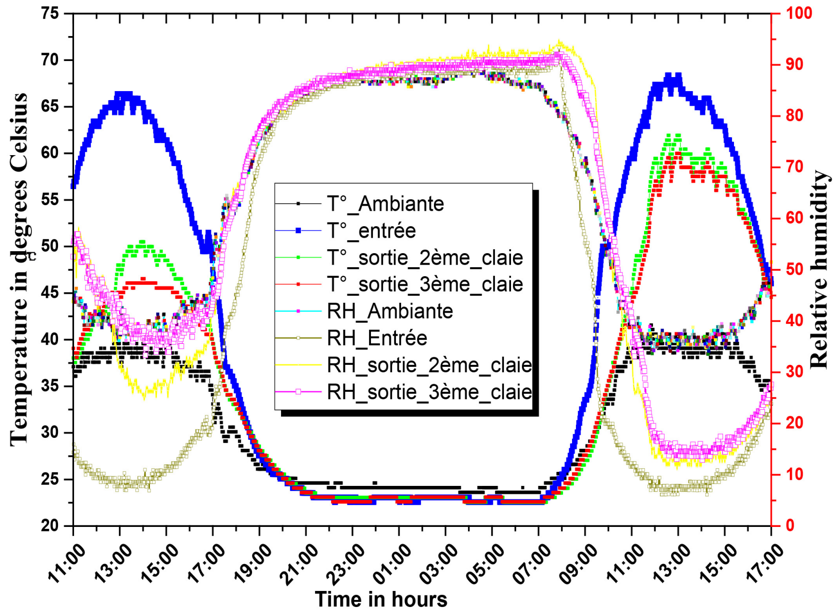

Figure 3. Performance comparison forced convection solar dryer vs. open air drying for bananas.

4.2. Comparison of Mass Losses of Bananas in a Solar Dryer and in Open Air

Figure 4 illustrates the variation in dry-base moisture content of bananas over time for different banana samples, both in a solar dryer and in open air. This drying process took place over two days, from an initial moisture content of 66% to a final moisture content of 32% (wet base). The mass losses recorded during drying allowed us to calculate the product's moisture content at each time point (Equation I-2). We observe the presence of only the decreasing phase, and the absence of the heating phase and the constant-rate phase for both drying methods. Comparison between these two drying methods revealed a faster drying rate in the solar dryer than in open air. The drying time is shorter in the solar dryer (15 hours) compared to 24 hours in open air.

This is because the temperature inside the dryer is higher, and this increased temperature promotes faster drying, leading to a shorter drying time. The moving dry air quickly removes water vapor, maintaining a concentration gradient favorable to moisture extraction. In contrast, the temperature is lower in the open air, and drying depends on wind speed, hence the slower drying process. Vapor remains localized around the samples, and moisture accumulates around the product, thus slowing down the drying process.

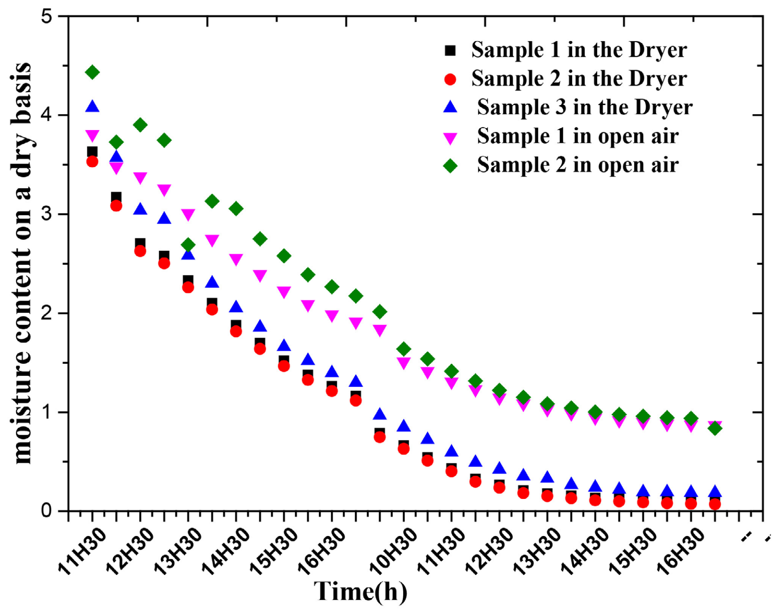

Figure 4. Variation in banana content over time.

4.3. Effect of Drying Air Temperature on Banana Desiccation

We have represented the evolution of temperature and humidity over time for the banana samples in the same figure (**Figure 5**). We observed that humidity decreases as temperature increases in all four figures (**Figures 5(a)-(d)**). It is noted that at the beginning of drying (first day), for temperatures ranging between 25˚C and 45˚C. A rapid decrease in moisture content was observed during the first six hours of drying, followed by a slowdown on the second day, despite temperatures varying between 45˚C and 65˚C. There was a disparity between the different banana samples at the drying rack level.

In **Figure 5(a)**, the temperature of tray 1 gradually increases on the first day from ~25˚C to ~50˚C. The moisture content decreases sharply in the first 6 hours. This is the initial phase, known as rapid drying, mainly due to the evaporation of free water (not bound to the substrate), which is readily accessible on the surface of the product. During the second day, despite the temperature at tray 1 of the solar dryer reaching 65˚C, the moisture content of the product decreases slowly, leading to a slowdown in drying. This phenomenon is explained by the fact that all the free water in the product has been removed, leaving only bound water, which is difficult to extract.

For **Figure 5(b)**, the temperature is unstable but generally increasing (fluctuating around 32˚C - 50˚C). The humidity of sample 2 (shelf 2) also decreases rapidly at first, then more slowly thereafter. The dynamics are the same as in (a). The temperature fluctuations may reflect an imbalance in solar heating or variations in airflow. This impacts the temperature gradient between the air and the product, and therefore the heat flux. During the second day, the maximum temperature at shelf 2˚C is 63˚C. However, the decrease in the product's moisture content is slowed due to the diffusion of water from the product's depths to the surface.

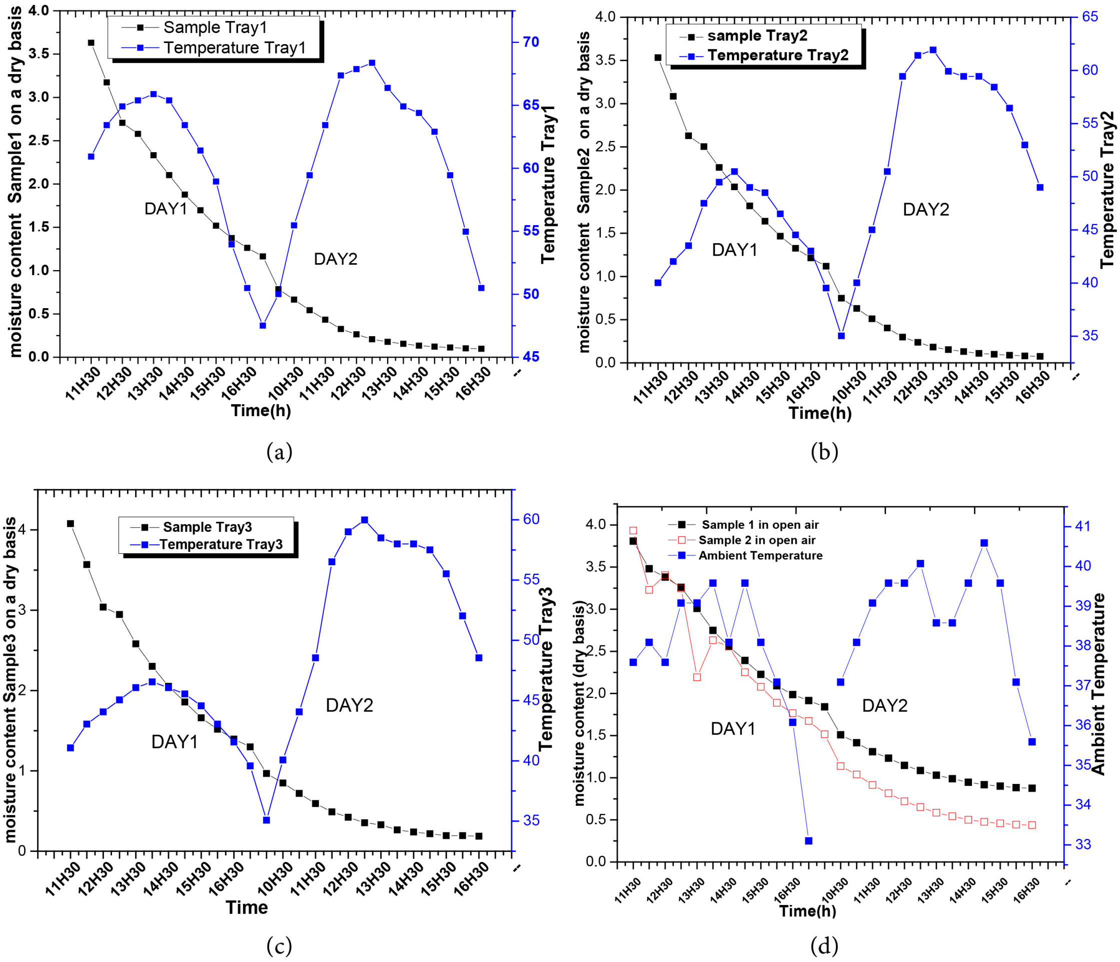

Figure 5. Influence of temperature on desiccation. (a) tray1; (b) tray2; (c) tray3; (d) open air.

For **Figure 5(c)**, the temperature is lower (~35˚C to ~45˚C), with some instabilities. The moisture content of sample 3 follows the same trend: a rapid initial decrease followed by stabilization. As the temperature increases, the vapor pressure gradient between the product surface and the air becomes greater, and evaporation accelerates. During the second day, the temperature of tray 3 reaches 60˚C. The decrease in relative humidity slows, marking the transition to phase 2 of the drying process.

For **Figure 5(d)**, all curves for samples 4 and 5 follow the same trend. The effect of temperature on humidity becomes less pronounced after 6 - 8 hours. The slow drying phase begins, where the predominant mechanism is the diffusion of bound water towards the product surface. This water is retained by physicochemical bonds (capillary, adsorbed, intracellular water).

4.4. Modeling of Drying Kinetics

Although Nine drying models were evaluated in the theoretical section, only the five best-fitting models were retained and presented in the results. These models were selected based on the most favorable statistical criteria: the highest adjusted

R^2 value, and the lowest RMSE and χ^2 values.

The drying kinetics of banana were studied by monitoring the evolution of moisture content over time, under the same experimental conditions as the other samples. The experimental data were fitted to these models using non-linear regression by the Levenberg-Marquardt method with Origin Pro 9.1 software. The model constants and the corresponding statistical criteria are presented in Table 3.

Table 3. Parameters and statistical results of the six models for banana.

	Samples	Model coefficients	χ^2	R^2	ESM
PAGE	**MR_1**	$n = 1.38305$ $k = 0.03817$	5.24244E−4	0.99447	0.00351
	MR_2	$n = 1.33257$ $k = 0.03741$	3.96287E−4	0.99567	0.00288
	MR_3	$k = 0.04135$ $n = 1.34984$	4.43637E−4	0.99524	0.0034
	MR_AMB1	$k = 0.05302$ $n = 1.05067$	7.50372E−4	0.98754	0.00495
	MR_AMB2	$k = 0.04774$ $n = 1.09389$	0.0017	0.97397	0.00688
NEWTON	**MR_1**	$k = 0.09757$	0.00364	0.96161	0.00392
	MR_2	$k = 0.08707$	0.00299	0.96731	0.00307
	MR_3	$k = 0.09722$	0.00315	0.96618	0.00363
	MR_AMB1	$k = 0.06087$	7.89091E−4	0.9869	0.00104
	MR_AMB2	$k = 0.06161$	0.00186	0.94758	0.00162
HENDERDERSON AND PABIS	**MR_1**	$A = 1.19155$ $k = 0.11579$	0.000111	0.98831	0.00351
	MR_2	$A = 1.16687$ $K = 0.1018$	8.21496E−4	0.99102	0.00258
	MR_3	$A = 1.19173$ $k = 0.11561$	6.23366E−4	0.99331	0.00262
	MR_AMB1	$A = 1.03869$ $k = 0.06383$	6.51661E−4	0.98918	0.00149
	MR_AMB2	$A = 1.06318$ $K = 0.06643$	0.00149	0.97709	0.0023
TWO-TERMS	**MR_1**	$A = 0.60118$ $B = 0.60119$ $k = 0.11853$ $g = 0.11853$	0.00162	0.98294	2874.62909
	MR_2	$A = 0.58924$ $B = 0.4952$ $k = 0.58924$ $g = 0.10459$	0.00124	0.98645	749.27199
	MR_3	$A = 0.60136$ $B = 0.60137$ $k = 0.11832$ $g = 0.11832$	9.67452E−4	0.98962	8735.33892

Continued

	MR_AMB1	$A = 1.06107$ $B = 1.21949E{-7}$ $k = 0.06822$ $g = -0.46508$	6.18551E−4	0.98973	0.00196
	MR_AMB2	$A = 1.0863$ $B = 1.09304E{-9}$ $k = 0.07093$ $g = -0.64402$	0.00149	0.97722	0.00281
LOGARITHMIC	**MR_1**	$A = 1.24429$ $C = -0.09974$ $k = 0.09355$	7.60377E−4	0.99199	0.00557
	MR_2	$A = 1.24975$ $C = -0.13331$ $k = 0.07816$	3.47319E−4	0.9962	0.01771 0.00366
	MR_3	$A = 1.23247$ $C = -0.07768$ $k = 0.09786$	4.22273E−4	0.99547	0.01611
	MR_AMB1	$A = 1.02597$ $C = 0.03699$ $k = 0.07208$	7.27992E−4	0.98792	0.00646
	MR_AMB2	$A = 1.05496$ $C = 0.03139$ $k = 0.07399$	0.00167	0.97444	0.05361

4.5. Analysis and Interpretation of the Table

The values of the correlation coefficient (R^2), of and the mean systematic values (MSV) of the six models shown in Table 1 allowed us, using the selection criteria stated in 2.1, to choose the page model for the banana samples in the dryer as the best model (Figure 6(a), Figure 6(b)) with:

$R^2 = 0.99447$ and ESM = 0.00351, $\chi^2 = 5.24244E{-4}$ (Sample 1)

$R^2 = 0.99876$ and ESM = 0.00288, $\chi^2 = 3.9628E{-4}$ (Sample 2)

$R^2 = 0.99524$ and ESM = 0.0034, $\chi^2 = 4.443637E{-4}$ (Sample 3)

For samples in open air, the Two_Termes model gave the best prediction (Figure 5(b)) with:

$R^2 = 0.98973$ and ESM = 0.00196, $\chi^2 = 6.18551E{-4}$ (Sample 4)

$R^2 = 0.97722$ and ESM = 0.00281, $\chi^2 = 1.49E{-3}$ (Sample 5)

Page's model (Figure 6(a)) exhibits a very high correlation coefficient R^2 (>0.994) for samples located in the dryer, indicating excellent correlation between experimental and modeled data. Very low χ^2 and ESM values reveal minimal prediction error.

For samples located outside, the Two-Terms model (Figure 6(b)) presents the best model because it combines two exponential functions, which allows it to express both the high initial speed of drying (at the beginning) and the slowing down of the process in the final phase.

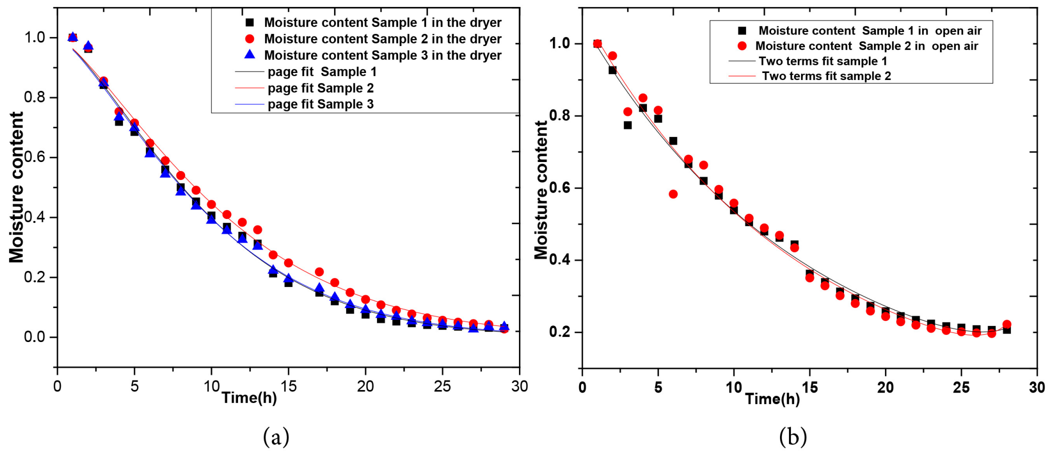

Figure 6. Comparison of the mathematical model of the banana. (a) Model page; (b) Model Two_Term.

4.6. Effective Diffusion of the Product

Figure 7 shows the variations in the logarithm of the different reduced moisture contents of the banana samples. This was achieved by plotting the variation of the logarithm of the experimental reduced moisture data as a function of time. This allowed us to obtain a slope with a slope coefficient. for all samples (Figure 7).

On the first day, the curves of log (MR) as a function of time are almost linear, indicating behavior close to Fickian diffusion. The R^2 values are very high (≈0.982 to 0.993), meaning that linear regression accurately explains the drying dynamics. Sample Ech3 has the best R^2 (0.993), suggesting superior drying regularity, perhaps due to better exposure to the hot airflow in the dryer. The samples in the dryer undergo faster and more homogeneous drying thanks to the effect of forced convection. The slope coefficients (values of k) are relatively high, meaning that moisture is extracted faster than in open air. This behavior is expected in a well-designed indirect solar dryer.

On the second day, the curves are less linear: a curvature is observed, particularly between 8 a.m. and 1 p.m., indicating a slowdown in drying. The R^2 values are also high (≈0.992 - 0.993), but the curve is not perfectly linear, meaning that other mechanisms are at play: nighttime cooling, variable humidity, and low air circulation. The slope is less steep than that of the samples in the dryer. Air drying is slower and less consistent, affected by weather conditions (wind, ambient humidity, radiation). The downward curvature suggests a decreasing drying phase where diffusion slows down (dry skin limiting water migration).

The effective diffusion coefficient (Deff) results for different banana samples are presented in Table 4. On dryer (Figure 7(a)) and open air (Figure 7(b)). The Deff coefficients range from 1.002E−8 to 9.621E−8 for samples dried in the dryer and from 8.93E−8 to 9.34E−8 for samples dried in the open air. This indicates a higher diffusivity for samples dried in the dryer than for samples dried in the open air. These results fall within the diffusivity range of 10^{-8} to 10^{-12} found in the literature for banana drying [5] and for agri-food products [14]-[16].

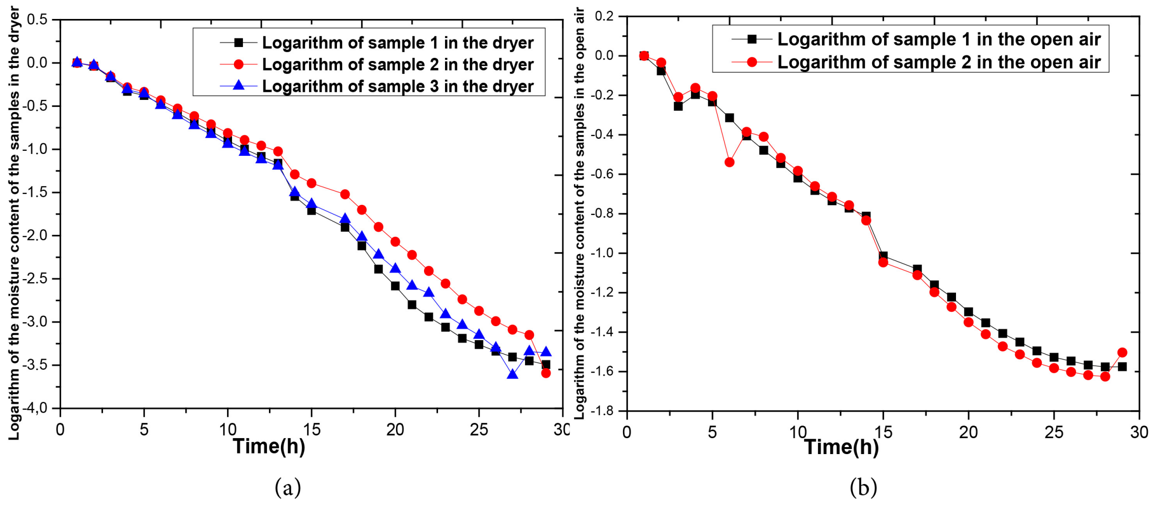

Figure 7. Logarithm of reduced humidity. (a) Dryer; (b) open air.

Table 4. Values of the effective diffusivity coefficients of the different samples.

Types	Sample	Deff (m²/s)	Slope	R^2	χ^2	ESM
Samples in the dryer	MR_1	9.150754e−08	−0.056446	0.982324	0.000887	0.029782
	MR_2	1.002562e−08	−0.061843	0.981517	0.001008	0.031753
	MR_3	9.622010e−09	−0.059353	0.992563	0.000391	0.019786
Samples in the open air	MR_AMB1	8.932170e−08	−0.055098	0.993073	0.000379	0.019458
	MR_AMB2	9.342621e−08	−0.057630	0.991649	0.000443	0.021038

5. Conclusion

The study of the solar drying kinetics of bananas demonstrates that drying using solar dryers improves upon traditional methods by protecting the produce and increasing performance. This technique, suitable for both domestic and industrial needs, is particularly effective in sunny regions. The results reveal kinetics characterized by a single decreasing phase, without a heating phase or a constant-rate phase. The Page and Two-Term models were identified as the most appropriate for describing drying in the dryer and in the open air, respectively, with uniform diffusivities between 10^{-12} and 10^{-8} m²/s. To optimize modeling, it is recommended to favour the Page model for controlled environments such as solar dryers, and to consider the use of the Two-Term model in contexts with climate variability, or even by coupling the latter with machine learning approaches to improve accuracy.

Acknowledgements

This study was conducted at the École Supérieure Polytechnique of Cheikh Anta Diop University in Dakar.

Conflicts of Interest

The authors declare no conflicts of interest regarding the publication of this paper.

References

[1] Charreau, A. and Cavaillé, R. Théorie et calculs. Techniques de l'Ingénieur, J2480. https://www.techniques-ingenieur.fr/base-documentaire/archives-th12/archives-operations-unitaires-genie-de-la-reaction-chimique-tiajb/archive-1/sechage-theorie-et-calculs-j2480/

[2] Harzig, J. (2001) Fruits and Vegetables and Nutritional Issues. *Professional Meeting*, No. 85, 4-6. https://agritrop.cirad.fr/485148/1/ID485148.pdf

[3] Talla, A., Puiggali, J.-R., Jomaa, W. and Jannot, Y. (2004) Shrinkage and Density Evolution during Drying of Tropical Fruits: Application to Banana. *Journal of Food Engineering*, **64**, 103-109. https://doi.org/10.1016/j.jfoodeng.2003.09.017

[4] Talla, A., Jannot, Y., Nkeng, G. and Puiggali, J.-R. (2004) Desorption Isotherms of Tropical Foodstuff. Application to Banana, Mango and Pineapple. *Drying Technology*, **23**, 1477-1498.

[5] Jannot, Y., Batsale, J., Ahouannou, C., Kanmogne, A. and Talla, A. (2002) Measurement Errors Processing by Covariance Analysis for an Improved Estimation of Drying Characteristic Curve Parameters. *Drying Technology*, **20**, 1919-1939. https://doi.org/10.1081/drt-120015576

[6] Jannot, Y., Talla, A., Nganhou, J. and Puiggali, J.-R. (2004) Modeling of Banana Convective Drying by the Drying Characteristic Curve (DCC) Method. *Drying Technology*, **22**, 1949-1968. https://doi.org/10.1081/drt-200032888

[7] Farias, R.P., Gomez, R.S., Silva, W.P., Silva, L.P.L., Oliveira Neto, G.L., Santos, I.B., *et al.* (2020) Heat and Mass Transfer, and Volume Variations in Banana Slices during Convective Hot Air Drying: An Experimental Analysis. *Agriculture*, **10**, Article No. 423. https://doi.org/10.3390/agriculture10100423

[8] Tasirin, S.M., Puspasari, I., Lun, A.W., Chai, P.V. and Lee, W.T. (2014) Drying of Kaffir Lime Leaves in a Fluidized Bed Dryer with Inert Particles: Kinetics and Quality Determination. *Industrial Crops and Products*, **61**, 193-201. https://doi.org/10.1016/j.indcrop.2014.07.004

[9] Benhamou, A., Idlimam, A., Lamharrar, A., Benyoucef, B. and Kouhila, M. (2008) Diffusivité hydrique et cinétique de séchage solaire en convection forcée des feuilles de marjolaine. *Journal of Renewable Energies*, **11**, 75-85. https://doi.org/10.54966/jreen.v11i1.58

[10] Mbengue, A., Gueye, M.S., Coly, M.L., Thiam, O.N. and Sow, M.L. (2020) Study of the Solar Drying of Bovine Meat: Drying Kinetics and Temperature Profiles in a Mixed Tunnel Solar Drier. *International Journal of Recent Advances in Multidisciplinary Research*, **7**, 6325-6333. http://ijramr.com/sites/default/files/issues-pdf/3318.pdf

[11] Coly, M.L., Mbaye, B.C., Gueye, M.S., Faye, W. and Diamanka, A. (2020) Fish Pre-Treated with Salt Brine: Process Study and Drying Kinetics. *International Journal of Advanced Research*, **8**, 35-44. https://doi.org/10.21474/ijar01/11820

[12] Wang, W., Li, M., Hassanien, R.H.E., Wang, Y. and Yang, L. (2018) Thermal Performance of Indirect Forced Convection Solar Dryer and Kinetics Analysis of Mango. *Applied Thermal Engineering*, **134**, 310-321. https://doi.org/10.1016/j.applthermaleng.2018.01.115

[13] Hamza, L., Mounir, K., Younes, B., Zakaria, T., Haytem, M., Hind, M., *et al.* (2020) Physicochemical Study of the Conservation of Moroccan Anchovies by Convective Solar Drying. *Renewable Energy*, **152**, 44-54. https://doi.org/10.1016/j.renene.2020.01.039

[14] Koua, K.B., Magloire, E.P. and Gbah, P. (2017) Drying of Cocoa Beans in an Indirect Solar Dryer with Forced Air Circulation. *Cames Applied Sciences and Engineering*, **2**, 15-19. https://publication.lecames.org/index.php/ing/article/view/1228

[15] Aregbesola, O.A., Ogunsina, B.S., Sofolahan, A.E. and Chime, N.N. (2015) Mathematical Modeling of Thin Layer Drying Characteristics of Dika (*Irvingia gabonensis*) Nuts and Kernels. *Nigerian Food Journal*, **33**, 83-89. https://doi.org/10.1016/j.nifoj.2015.04.012

[16] Samimi-Akhijahania, H. and Arabhosseinib, A. (2018) Accelerating Drying Process of Tomato Slices in a PV-Assisted Solar Dryer Using a Sun Tracking System. *Renewable Energy*, **123**, 428-438.